Cell Host & Microbe, Volume *13*

Supplemental Information

The Antiviral Effector IFITM3 Disrupts Intracellular Cholesterol Homeostasis to Block Viral Entry

Samad Amini-Bavil-Olyaee, Youn Jung Choi, Jun Han Lee, Mude Shi, I-Chueh Huang, Michael Farzan, and Jae U. Jung

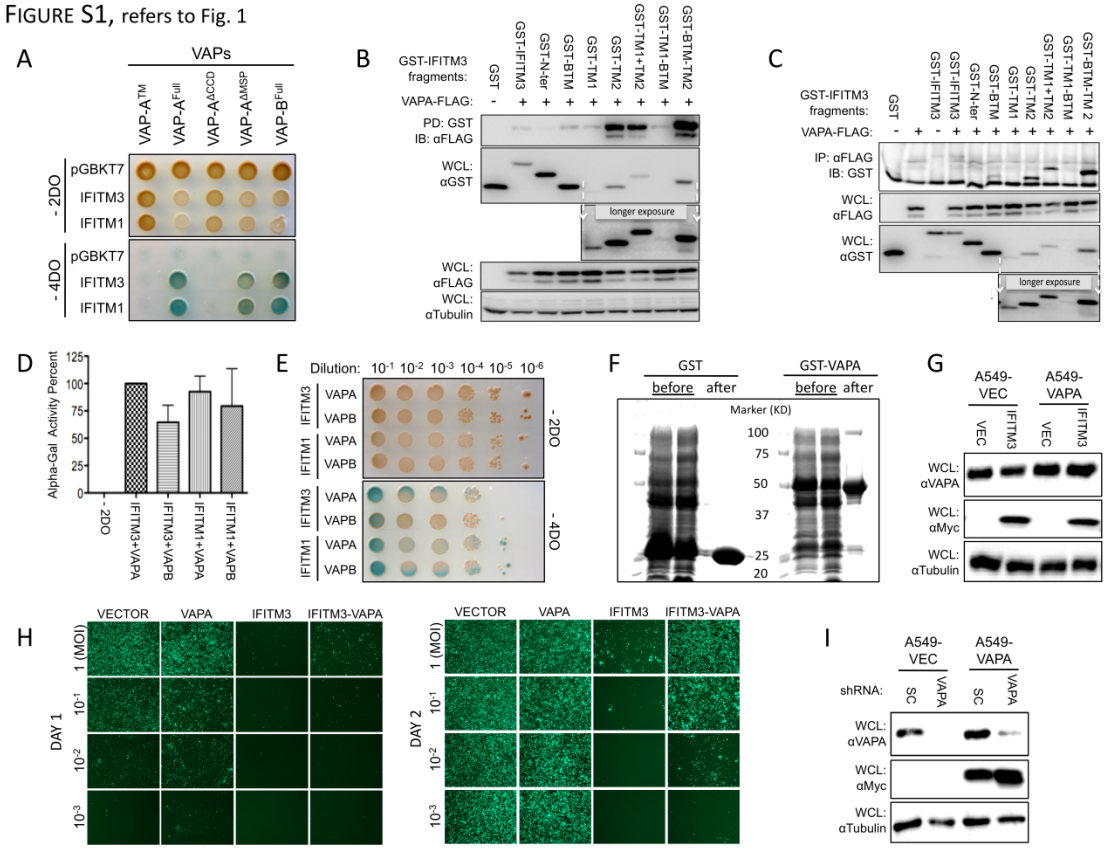

Figure S1, Related to Figure 1. Y2H, IP and GST pull-down assays to demonstrate the interaction between the IFITM3 TM2 region with the VAPA CCD-TM region; IFITM3 and VAPA expression and VSV replication

(A) Y2H assay was performed to test the interaction of IFITM1 (cloned in pGBKT7 vector) and IFITM3 (cloned in pGBKT7 vector) with VAPA and VAPB full-length and mutant forms (cloned in pACT2.1 vector).

(B and C) HEK-293T cells were co-transfected with different fragments of the GST-IFITM3 fusion (cloned in pEBG vector) and VAPA-FLAG (cloned in pCDH vector). At 2 days posttransfection, cells were subjected to IP with anti-FLAG antibody or GST pull-down, and then IB with the indicated antibodies.

(D) AH109 yeast carrying bait (IFITM3 or IFITM1) and target (VAPA or VAPB) were grown in -2DO media (-His –Leu) at 30°C, 200 rpm. At OD=2.0, 1mL of yeast cultures were centrifuged and supernatants were subjected to Alpha-Gal activity according to Sigma enzymatic assay of alpha-Galactosidase (EC 3.2.1.22). Values represent mean ± SD, n ≥ 3 independent experiments.

(E) Y2H assay was performed to test the interaction of VAPA and VAPB proteins with IFITM1 and IFITM3.

(F) Coomassie Blue staining of bacterially purified GST (~25KD) and GST-VAPA (~50KD) proteins before and after purification.

(G) A549 cells were used for IB assay to show the levels of IFITM3 and VAPA expression.

(H) A549 cells were infected with various MOIs of GFP-VSV. At day 1 and 2 postinfection, cells were photographed using immunofluorescence microscope (magnification: 4x).

(I) A549-Vector and A549-IFITM3 cell lines were infected with lentivirus carrying either VAPA-shRNA (VAPA) or SC-shRNA (SC). After two days, A549 cells were used for IB assay to show the levels of IFITM3 and VAPA expression.

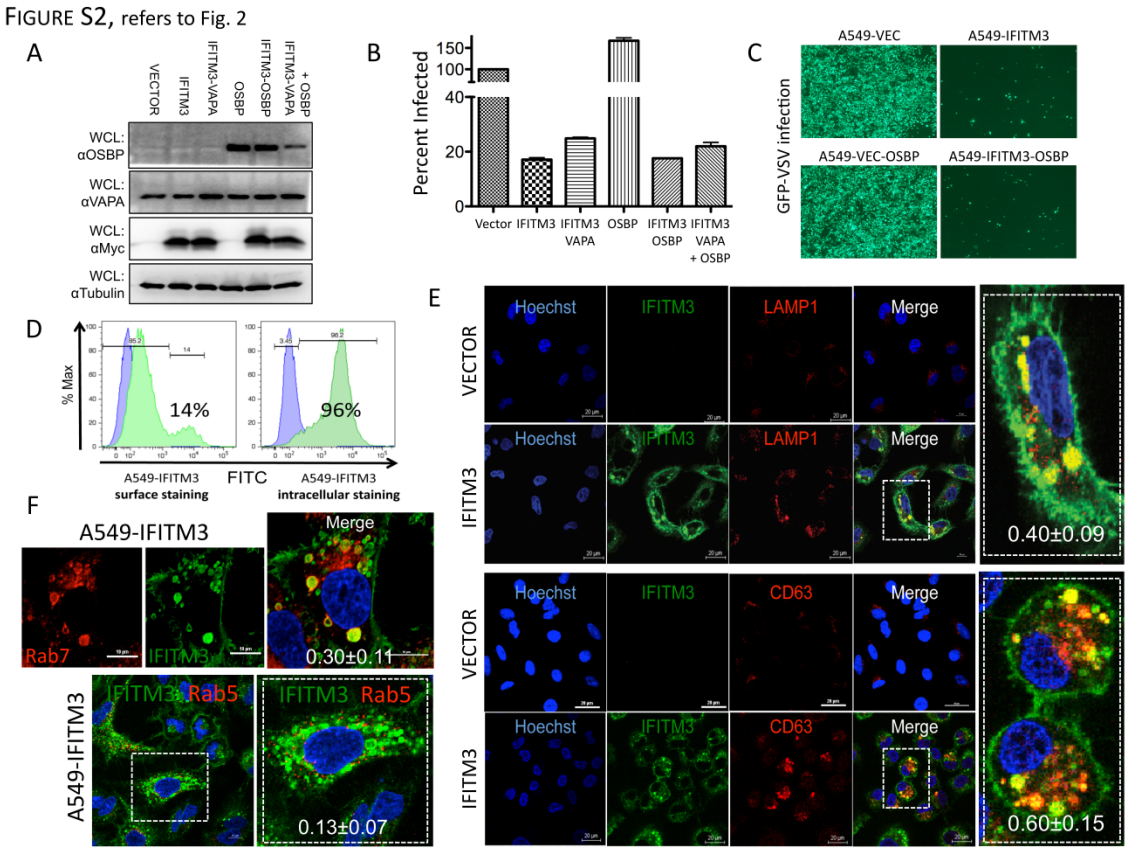

Figure S2, Related to Figure 2. Effect of OSBP expression on viral entry and IFITM3 localization

(A) A549 cells were used for IB assay to show the levels of OSBP, VAPA and IFITM3-Myc expression.

(B) A549-Vector, A549-IFITM3, A549-IFITM3-VAPA, A549-OSBP, A549-IFITM3-OSBP and A549-IFITM3-VAPA+OSBP cells were subjected to viral single-entry assay using defective MLV-EGFP pseudotyped with VSV glycoprotein (gp). Values represent mean ± SD, n ≥ 3 independent experiments.

(C) A549-Vector, A549-IFITM3, A549-OSBP and A549-IFITM3-OSBP cells were infected with GFP-VSV, after 2 days postinfection, cells were photographed by immunofluorescence microscope (magnification: 4x).

(D) A549-IFITM3 cells were used for flow cytometry analysis using anti-Myc antibody. For flow cytometry analysis, cells were permeabilized with or without saponin prior to staining with antibody.

(E) A549-Vector and A549-IFITM3 cells were fixed and immune-stained with anti-Myc (IFITM3), anti-LAMP1 or anti-CD63 antibody, followed by confocal microscopy analysis. Scale bar: 20μm. Magnified images of the inserts are shown in the right panels. The LAMP1-IFITM3 (0.40±0.09) and CD63-IFITM3 (0.60±0.15) colocalization efficiency was calculated by Pearson's correlation coefficient (mean ± SD, $n \geq 20$ cells).

(F) A549-IFITM3 cells were fixed and immune-stained with anti-Myc (IFITM3), anti-Rab7 or anti-Rab5 antibodies, followed by confocal microscopy analysis. Scale bar: 10μm. Magnified image of the insert is shown in the right panel. The Rab7-IFITM3 (0.30±0.11) and Rab5-IFITM3 (0.13±0.07) colocalization efficiency was calculated by Pearson's correlation coefficient (mean ± SD, $n \geq 20$ cells).

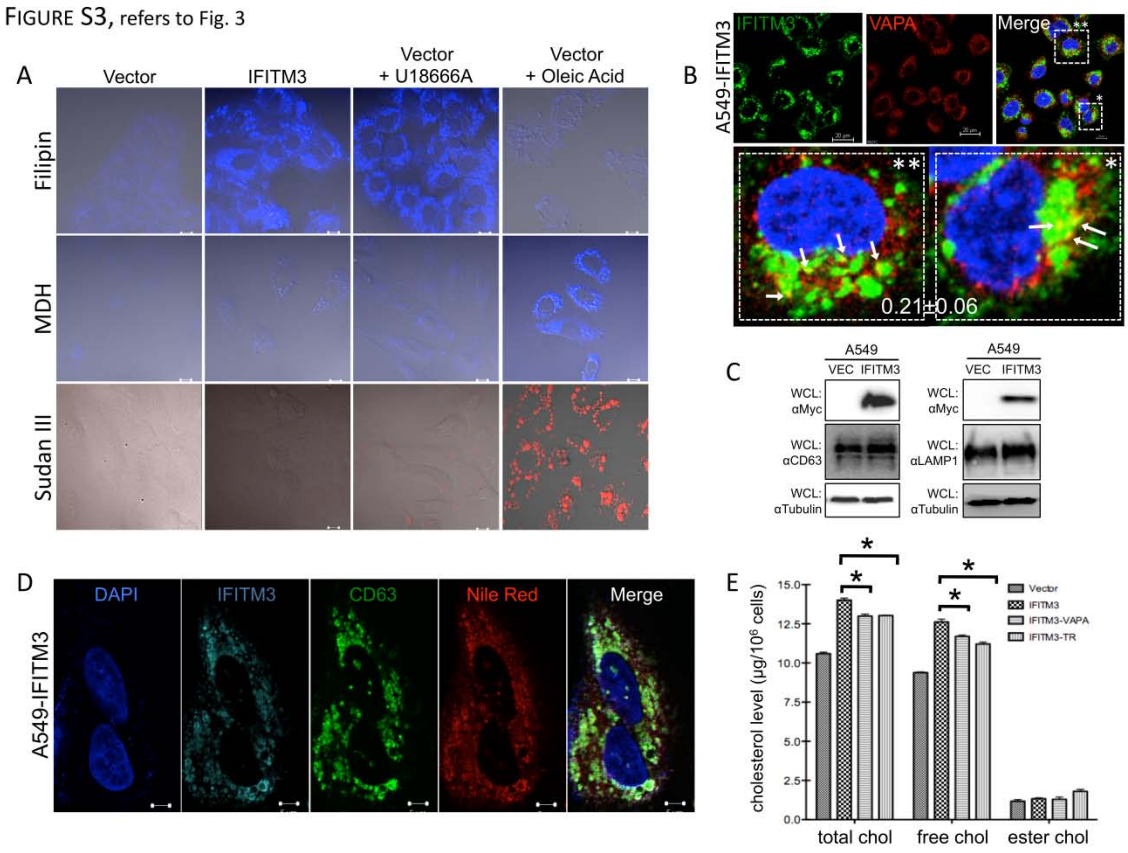

Figure S3, Related to Figure 3. Lipid droplet staining, cholesterol quantification and IFITM3 and VAPA localization

(A) A549-Vector cells were treated with either U18666A (to induce cholesterol-laden endosomal compartments) or Oleic acid (to induce lipid droplet vacuoles). Afterward, A549-Vector, A549-IFITM3, U18666A-treated A549-Vector and Oleic acid treated A549-Vector cells were fixed and subjected for confocal microscopy study. Cells were stained with Filipin (a polyene macrolide antibiotic to stain free cholesterols), MDH (a fluorophore molecule to stain lipid droplets) and Sudan III (a lysochrome to stain triglycerides-containing compartments as lipid droplet vacuoles). Scale bar: 10μm.

(B) A549-IFITM3 cells were fixed and immune-stained with anti-Myc (IFITM3) and anti-VAPA, followed by confocal microscopy analysis. Scale bar: 20μm. Magnified images of two inserts (indicated with asterisk) are illustrated in the two below panels. Colocalization between VAPA and IFITM3 was quantified as 0.21±0.06 (Pearson's coefficient, mean ± SD, n ≥ 20 cells).

(C) WCLs of A549-Vector and A549-IFITM3 were analyzed by immunoblotting with the indicated antibodies.

(D) A549-IFITM3 cells were fixed and immune-stained with anti-Myc (IFITM3, Alexa Fluor-633, pink color), anti-CD63 antibody (Alexa Fluor-488, green color), and Nile Red (Red color). DAPI (blue color) was used to stain nucleus. Scale bar: 5μm.

(E) Total (total chol), free (free chol) and esterfied (ester chol) cholesterols were quantified in the indicated cells using the Cholesterol Quantification Kit. Values represent mean ± SD, n = 3 independent experiments. Significant differences (*p-value* < 0.05) compared to IFITM3 are marked by asterisk.

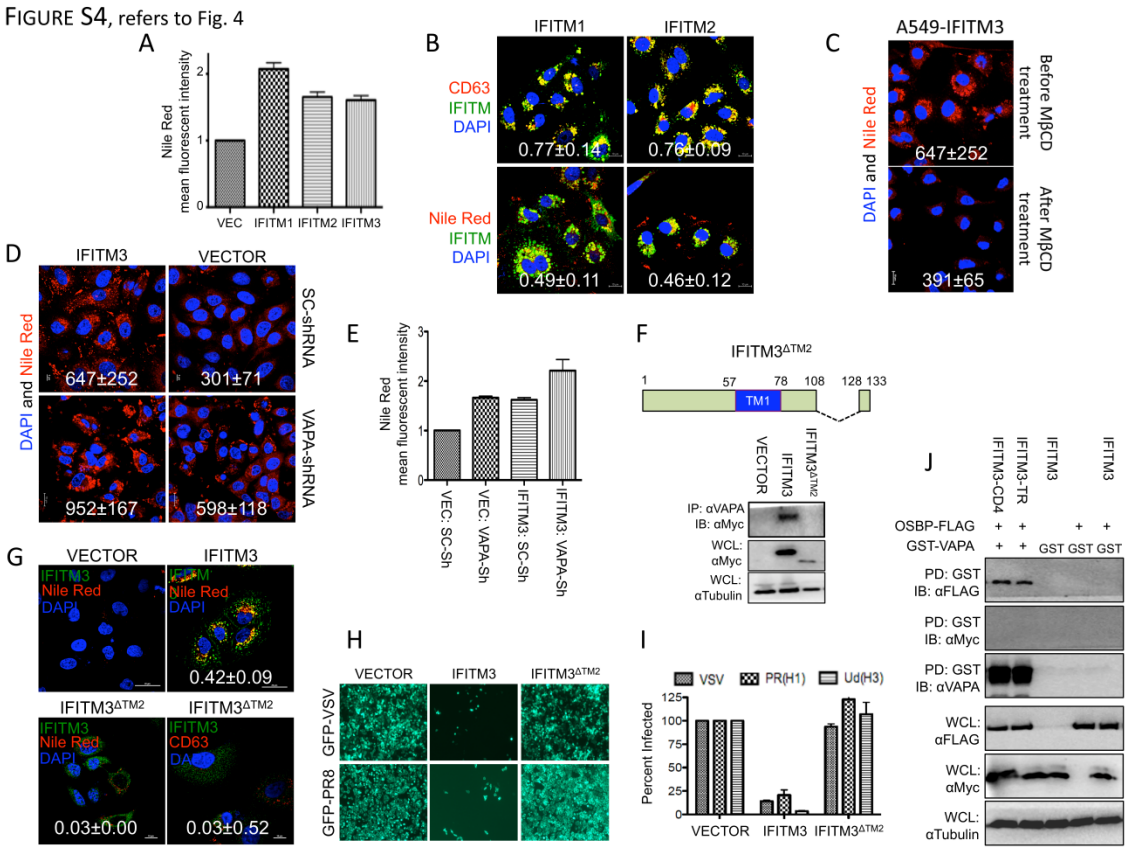

Figure S4, Related to Figure 4. Effect of IFITM and VAPA expression on intracellular cholesterol levels, and the IFITM3 TM2 is required for the restriction of viral entry

(A) A549-Vector, A549-IFITM1, A549-IFITM2, and A549-IFITM3 cells were stained with Nile Red dye to measure their intracellular cholesterol levels by flow cytometry. The mean fluorescence intensities (MFIs) were compared and presented as relative folds compared with those of A549-Vector cells. Values represent mean ± SD, n ≥ 3 independent experiments.

(B) A549-IFITM1 or A549-IFITM2 cells were stained with CD63, Nile Red and together with anti-Myc (IFITM1/2). Cell images were captured using confocal microscopy. Scale bars: 10μm. The metric values (mean ± SD) correspond to the quantitative assessment of the colocalization of CD63 with IFITM1/2 or Nile Red with IFITM1/2 calculated by Pearson's correlation coefficient (n ≥ 20 cells).

(C) A549-IFITM3 cells were fixed and stained with Nile Red dye before and after MβCD treatment. Images were captured using confocal microscopy. Scale bar: 10μm. The metric

values represent the Nile Red fluorescence intensity before and after MβCD treatment (mean ± SD, n ≥ 20 cells).

(D) A549-Vector and A549-IFITM3 were infected with VAPA-shRNA lentivirus or SC-shRNA lentivirus. At 48hrs postinfection, cells were fixed, stained with Nile Red dye and subjected to confocal microscopy analysis. Scale bar: 5μm. The metric values represent the Nile Red fluorescence intensity (mean ± SD, n ≥ 20 cells).

(E) A549-Vector and A549-IFITM3 were infected with VAPA-shRNA lentivirus or SC-shRNA lentivirus. At 48hrs postinfection, cells were fixed, stained with Nile Red dye and subjected to flow cytometry analysis. Values represent mean ± SD, n = 3 independent experiments.

(F) Schematic diagram of the IFITM3 $^{\Delta TM2}$ mutant, and A549 cells were used for IP and IB assays by the indicated antibodies.

(G) A549-Vector, A549-IFITM3 and A549-IFITM3$^{\Delta TM2}$ cell lines were fixed and stained with Nile Red dye, anti-Myc antibody and anti-CD63 antibody for confocal microscopy. DAPI was used for nucleus staining. Scale bar: 20μm. The metric values (mean ± SD) denote the quantitative assessment of the colocalization between Nile Red and IFITM3 WT (0.42±0.09) or IFITM3$^{\Delta TM2}$ mutant (0.03±0.00) or between CD63 and IFITM3$^{\Delta TM2}$ mutant (0.03±0.52) (Pearson's coefficient, mean ± SD, n ≥ 20 cells).

(H) A549-Vector, A549-IFITM3 and A549-IFITM3$^{\Delta TM2}$ cells were infected with GFP-VSV and GFP-PR8 influenza virus (MOI=1.0). After two days postinfection, cells were photographed using fluorescence microscopy (magnification: 10x).

(I) A549-Vector, A549-IFITM3 and A549-IFITM3$^{\Delta TM2}$ cells were subjected to viral single-entry assay using defective MLV-EGFP pseudotyped with envelope proteins of VSV, IAV H1N1 (PR8), and IAV H3N1 (Udorn). Values represent mean ± SD, n ≥ 3 independent experiments.

(J) Bacterially purified GST or GST-VAPA proteins were mixed with OSBP-containing cell lysates together with IFITM3-, IFITM3-CD4- or IFITM3-TR-containing cell lysates. After 2 hours incubation at 4°C, GST pull-down (GST PD) and IB were performed with the indicated antibodies. WCLs were used for IB with the indicated antibodies.

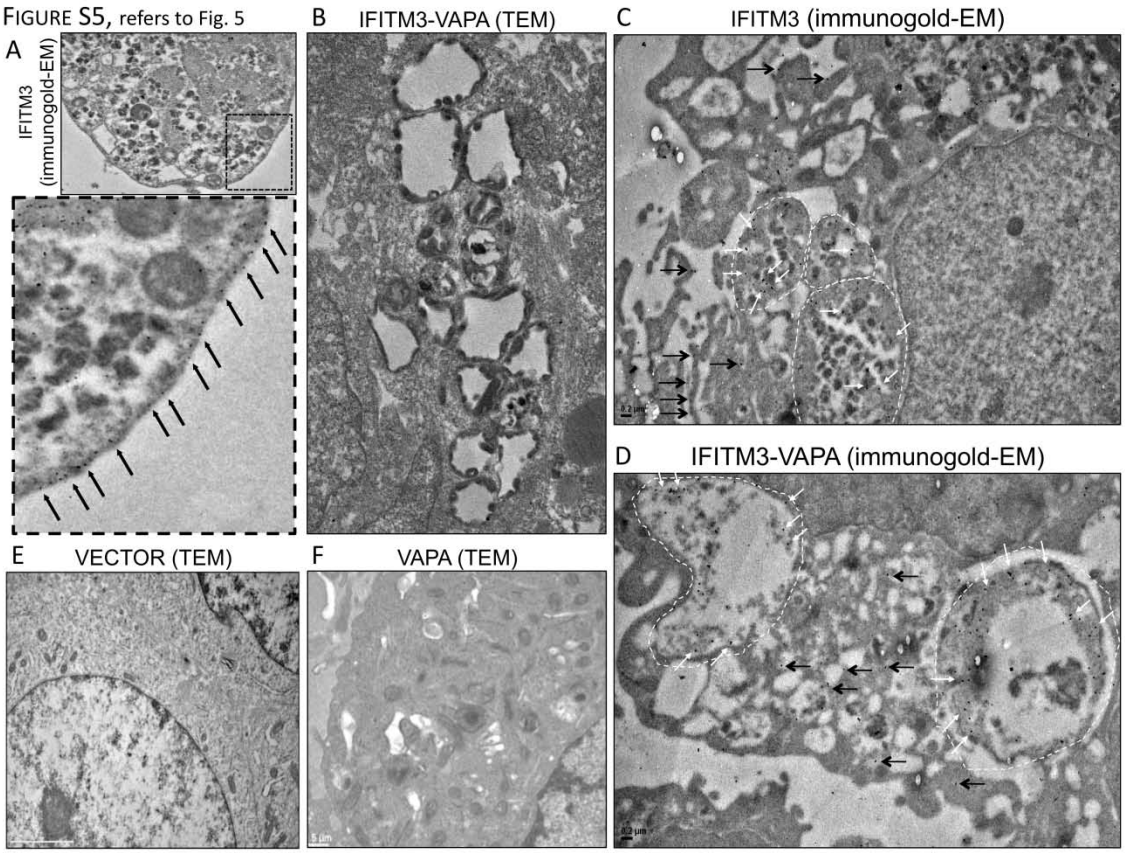

Figure S5, Related to Figure 5. Immunogold and TEM of A549-IFITM3 and A549-IFITM3-VAPA cells; Immunogold EM of VAPA in A549-IFITM3 and A549-IFITM3-VAPA cells and TEM of A549-Vector and A549-VAPA cells

(A) Ultrathin sections of L. R. White-embedded A549-IFITM3 cells were subjected to immunolabeling using anti-Myc antibody (IFITM3), followed by staining with 15nm-gold particle-conjugated secondary antibody. The bottom panel is an enlarged insert and the arrows in the bottom panel indicate plasma membrane localization of IFITM3. Scale bar: 0.2μm.

(B) TEM images of ultrathin sections of epon-embedded A549-IFITM3-VAPA cells were captured. Scale bar: 0.2μm.

(C-D) A549-IFITM3 and A549-IFITM3-VAPA cells were fixed and ultrathin sections of L. R. White-embedded cells were subjected to immunolabeling with anti-VAPA antibody and 15nm-gold particle-conjugated secondary antibody. The black arrows indicate ER localization of VAPA and the white arrows indicate endosomal localization of VAPA. Scale bar: 0.2μm.

(E) TEM images of ultrathin sections of epon-embedded A549-Vector cells were captured. Scale bar: 2μm.

(F) TEM images of ultrathin sections of epon-embedded A549-VAPA cells were captured. Scale bar: 0.5μm.

FIGURE S6, refers to Fig. 6

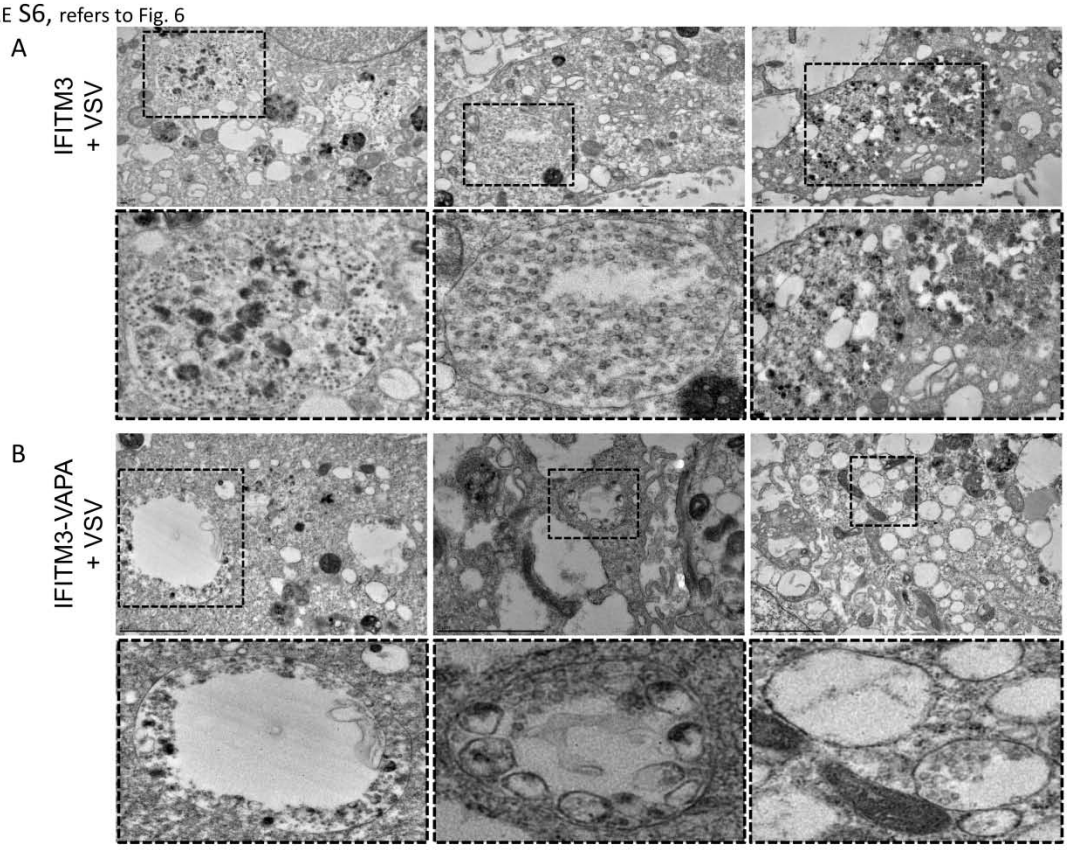

FIGURE S6, CONTINUED

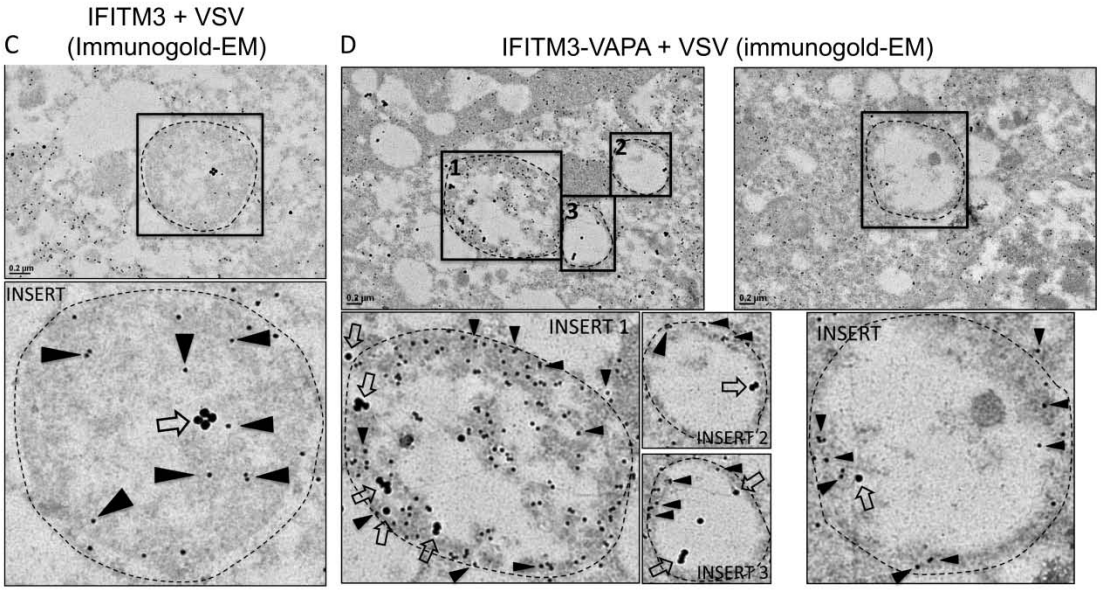

Figure S6, Related to Figure 6. TEM of A549-IFITM3 and A549-IFITM3-VAPA upon VSV infection; Immunogold EM of IFITM3 and VSVgp in A549-IFITM3 and A549-IFITM3-VAPA upon VSV infection

(A) TEM images of ultrathin sections of epon-embedded A549-IFITM3 cells after VSV infection were captured. The bottom panels are magnified inserts of the top panels. Scale bar: 0.2μm.
(B) TEM images of ultrathin sections of epon-embedded A549-IFITM3-VAPA cells after VSV infection were captured. The bottom panels are magnified images of the inserts of the top panels. Scale bar: 2μm.
(C) Ultrathin sections of L.R. White-embedded VSV-infected A549-IFITM3 cells were subjected to dual-immunogold labeling. Black triangular arrows indicate 15nm gold-conjugated anti-Myc-labeled IFITM3, and the empty arrows indicate 30nm gold-conjugated anti-VSVgp-labeled VSV glycoprotein. The bottom panel is magnified image of the insert of the top panel. Scale bar: 0.2μm.

(D) Ultrathin sections of L.R. White-embedded VSV-infected A549-IFITM3-VAPA cells were subjected to dual-immunogold labeling. Black triangular arrows indicate 15nm gold-conjugated anti-Myc-labeled IFITM3, and the empty arrows indicate 30nm gold-conjugated anti-VSVgp-labeled VSV glycoprotein. The bottom panels are magnified images of the inserts of the top panels. Scale bar: 0.2μm.

SUPPLEMENTAL EXPERIMENTAL PROCEDURES

Yeast two-Hybrid (Y2H) screening

To map the binding domains of IFITM3 and VAPA, various fragments of the *VAPA* gene were PCR-amplified and cloned into the *EcoRI-XhoI* site of the pACT2 vector and transformed to the AH109 yeast expressing full-length *IFITM3*. Conversely, various fragments of the *IFITM3* gene were PCR-amplified and cloned into the *NdeI-BamHI* site of the pGBKT7 vector. These constructs were used for interaction mapping in AH109 cells.

Transfection of IFITM3, VAPA and OSBP

Puromycin resistant A549-IFITM3 and A549-vector infected cells with lentivirus carrying pCDH-MCS-EF1-Neo-VAPA or -VAPA-FLAG were selected by G418 (Sigma, Saint Louis, MI) resistance followed by single cell colony isolation to obtain A549-IFITM3-VAPA and A549-vector-VAPA cells. The *OSBP* cDNA (BC011581) was purchased (Open Biosystems), PCR-amplified and clone into the *NheI-BamHI* site of the lentivector pCDH-MCS-EF1-Hygro (System Biosciences), transduced into A549-vector, A549-IFITM3 and A549-IFITM3-VAPA cells, followed by Hygromycin B (Invitrogen) selection.

Cell culture, immunoblotting, immunoprecipitation and Glutathione S-transferase (GST) pull-down

Antibodies used for WB and IP were anti-rabbit VAPA, clone H-40 (Santa Cruz Biotechnology, Santa Cruz, CA); anti-mouse 9E10 and anti-rabbit Myc (Covance, Emeryville, CA); anti-mouse and anti-rabbit FLAG (Sigma); anti-mouse ϒ-Tubulin (Sigma); anti-mouse and anti-rabbit GST (Covance); anti-mouse CD63, clone MX-49.129.5 (Santa Cruz Biotechnology); anti-mouse LAMP1 (abcam, Cambridge, UK), anti-rabbit OSBP (#11096-1-AP, proteintech, Chicago, IL) and anti-rabbit IgG (EMD Millipore, Billerica, MA). For mapping study in mammalian cell, different fragments of the *IFITM3* gene were PCR-amplified and cloned into *BamHI-NotI* of the pEBG mammalian expression vector. The 293T cells were transfected and used for GST-PD study, followed by WB analysis with the indicated antibodies. Briefly, for IP and GST-PD assays, cells were lysed in lysis buffer (1% NP40, 50mM Tris-HCl pH 7.5, 150mM NaCl, 1mM EDTA) plus protease inhibitor cocktail (Roche). After pre-clearing of cell lysates with Sepharose beads (GE Healthcare Life Sciences), target proteins were immunoprecipitated by incubation either with the indicated antibodies and protein A agarose beads (GE Healthcare Life Sciences) or

with GST beads (GE Healthcare Life Sciences). Immune complexes or GST complexes were washed with lysis buffer, resolved by SDS-PAGE and analyzed by immunoblotting.

VAPA cDNA was PCR-amplified and cloned into the *BamHI-XhoI* site of the pGEX-6P-1 bacterial expression vector (GE Healthcare Life Sciences), and GST and GST-VAPA proteins were purified using GST beads based on manufacturer protocol. To show the interaction between VAPA and OSBP or VAPA and IFITM3 in the presence of increasing amounts of IFITM3 or OSBP, cells were lysed in lysis buffer and then pre-cleared with Sepharose beads. Bacterially purified GST-VAPA protein (~3μg) was added to A549-vector, A549-IFITM3, or A549-OSBP cell extracts (Ext), followed by GST-PD at 4°C for 2 hours. GST beads were washed several times with lysis buffer and subjected to immunoblotting with indicated antibodies.

VAPA shRNA silencing

To generate recombinant shRNA-lentiviruses, 293T cells were transfected with either pLKO.1-TRC-VAPA-shRNA (ccgg gcg tat ttg aaa tgc cca atg ctcgag cat tgg gca ttt caa ata cgc tttttg) or pLKO.1-TRC-SC-shRNA vector together with packaging vectors including psPAX2/gag-pol and MACHgp. A549-vector and A549-IFITM3 cells were infected with indicated recombinant lentiviruses carrying VAPA-shRNA or scramble (SC)-shRNA and VAPA levels were examined by immunoblotting analysis.

Influenza virus and VSV infection

VSV was concentrated by ultra centrifugation and purified using linear sucrose gradient centrifugation as described previously (Cureton et al., 2010), aliquoted and kept at -80°C for some experiments. A549-vector, A549-IFITM3, A549-VAPA, and A549-IFITM3-VAPA cells were infected by IAV or VSV and viral replications were determined using standard plaque forming unit (PFU) assay. After VAPA down-regulation in A549-vector and A549-IFITM3, cells were infected with influenza and VSV viruses, and viral infection was determined by standard plaque assay.

Defective MLV-EGFP pseudotyped virus production and entry assay

At 48hrs postinfection with defective MLV-EGFP pseudotyped viruses, A549-vector, A549-IFITM3, A549-VAPA and A549-IFITM3-VAPA cells were subjected to flow cytometry analysis to determine the EGFP positive cell population as previously described (Brass et al., 2009). Entry

assay was also performed upon treatment with methyl-beta-cyclodextrin, MβCD (Sigma) to deplete intracellular cholesterol.

Confocal, immunofluorescence microscopy, colocalization analysis and cholesterol quantification

Antibodies that used for confocal analysis were: anti-mouse 9E10 (Covance); anti-rabbit Myc (abcam, Cat. #ab9106); anti-mouse CD63 clone MX-49.129.5 (Santa Cruz Biotechnology); anti-mouse LAMP1, clone H-228 (Santa Cruz Biotechnology); anti-mouse LBPA (Echelon Biosciences, Salt Lake City, UT); anti-rabbit VAPA, clone H-40 (Santa Cruz Biotechnology); anti-mouse Rab7, clone Rab7-117 (abcam); anti-mouse Rab5, clone D11 (Santa Cruz Biotechnology). Anti-mouse and/or anti-rabbit Alexa Fluor-488, Alexa Fluor-568 and Alexa Fluor-633 (Invitrogen) were used as secondary antibodies. Hoechst or DAPI (Invitrogen) was used to stain nucleus. Filipin (Sigma) was used to stain free cholesterols in cells. Nile Red (Enzo Life Sciences) was used to stain cholesterol and lipid droplet in cells. Monodansylpentane (MDH) (Abgent Inc. San Diego, CA) and Sudan III (Sigma) were used to stain lipid droplet (Velikkakath et al., 2012; Yang et al., 2012). To induce cholesterol-laden endosomal compartments and lipid droplet vacuoles, A549 cells were treated with 2 μg/ml U18666A (Sigma) and 0.2 mM Oleic acid (Sigma), respectively. In brief, cells were stained with 0.1 mg/ml Filipin for 2 hours, 100 μM MDH for 15 min, 2 mg/ml filtered-Sudan III in 70% ethanol or 1 μM Nile Red for 10 min. Nile Red staining was also used for flow cytometry analysis to quantify cholesterol level as described (Schaedlich et al., 2010). Also, total-, free- and esterified-cholesterols were quantified using Cholesterol Quantification Kit (Sigma-Aldrich) according to manufacture's instruction. To quantify colocalization of proteins, the Pearson's correlation coefficients of the different fluorescent signals were determined with the NIS-Elements Advanced Research (AR) imaging software, version 3.22.11 (Nikon Instruments Inc. Melville, NY) based on the pixel density and overlap of two-color signals. The mean ± SD of the Pearson's correlation coefficient value was calculated based on more than 20 cells and the metric values were presented in each image. To calculate the intensity of the Nile Red staining, more than 20 cells were analyzed using the NIS-Elements AR software. To monitor replication of GFP-VSV and GFP-IVA within infected A549 cells, GFP fluorescence signal was captured by immunofluorescence microscopy (Olympus 1X71 Inverted Microscope).

Electron microscopy

Briefly, the transduced cells with or without VSV infection (MOI ~250, 1 hour infection) were fixed by ½K and then osmium tetroxide solutions. After staining with uranium salt and dehydration steps, cells were treated with propylene oxide, infiltrated with Epon plastic (TED PELLA, Redding, CA) and then embedded into the Epon blocks. After Epon polymerization, ultra-thin sections were prepared using an ultra-microtome apparatus (MT6000, Servall) and sections were loaded on 300 mesh grids. TEM images were captured by a JEOL JEM 2100 electron microscope. The L. R. White procedure was used for immunoelectron microscopy. Briefly, after fixation of samples with Ψ fixation solution, samples were dehydrated, and then infiltrated by L.R. White resin (Electron Microscopy Sciences, Hatfield, PA). Cells were embedded into the capsules and polymerized. Ultra-thin sections were prepared and sections were loaded on 300 mesh cupper grids. Samples were probed with anti-mouse 9E10 (Covance); anti-rabbit Myc (abcam, Cat. #ab9106), anti-mouse VSV-G, clone P5D4 (Sigma, Cat. #V5507), or anti-VAPA antibody. Anti-mouse and anti-rabbit antibodies conjugated with 30 nm-nano-gold and 15 nm-nano-glod particles (BBInternational, Cardiff, UK) were used as secondary antibodies. After washing steps, cells were stained with uranium salt, and images were captured by the electron microscope (JEOL JEM 2100).

SUPPLEMENTAL REFERENCES

Brass, A.L., Huang, I.C., Benita, Y., John, S.P., Krishnan, M.N., Feeley, E.M., Ryan, B.J., Weyer, J.L., van der Weyden, L., Fikrig, E.*, et al.* (2009). The IFITM proteins mediate cellular resistance to influenza A H1N1 virus, West Nile virus, and dengue virus. Cell *139*, 1243-1254.

Cureton, D.K., Massol, R.H., Whelan, S.P., and Kirchhausen, T. (2010). The length of vesicular stomatitis virus particles dictates a need for actin assembly during clathrin-dependent endocytosis. PLoS Pathog *6*, e1001127.

Schaedlich, K., Knelangen, J.M., Navarrete Santos, A., and Fischer, B. (2010). A simple method to sort ESC-derived adipocytes. Cytometry A *77*, 990-995.

Velikkakath, A.K., Nishimura, T., Oita, E., Ishihara, N., and Mizushima, N. (2012). Mammalian Atg2 proteins are essential for autophagosome formation and important for regulation of size and distribution of lipid droplets. Mol Biol Cell *23*, 896-909.

Yang, H.J., Hsu, C.L., Yang, J.Y., and Yang, W.Y. (2012). Monodansylpentane as a blue-fluorescent lipid-droplet marker for multi-color live-cell imaging. PLoS One *7*, e32693.